Electrostatic (plasmon) resonances in nanoparticles

Isaak D. Mayergoyz
Department of Electrical and Computer Engineering, Institute for Advanced Computer Studies, University of Maryland, College Park, Maryland 20742, USA

Donald R. Fredkin
Department of Physics, University of California, San Diego, La Jolla, California 92093, USA

Zhenyu Zhang
Department of Electrical and Computer Engineering, Institute for Advanced Computer Studies, University of Maryland, College Park, Maryland 20742, USA

(Received 12 April 2005; revised manuscript received 3 August 2005; published 14 October 2005)

A surface integral eigenvalue based technique for the direct calculation of resonance values of the permittivity of nanoparticles, and hence resonance frequencies, is discussed. General physical properties of electrostatic (plasmon) resonances are presented. Strong orthogonality properties of resonance modes, a two-dimensional phenomenon of "twin" spectrum and explicit estimates of resonance frequencies in terms of geometrical characteristics of convex nanoparticles are reported. Second-order corrections for resonance values of the dielectric permittivity are derived. Tunability and optical controllability of plasmon resonances in semiconductor nanoparticles are discussed and, as a digression, a plausible plasmon resonance mechanism for nucleation and formation of ball lightning is outlined. An efficient numerical algorithm for the calculation of resonance frequencies is developed and illustrated by extensive computational results that are compared with theoretical results and available experimental data.

DOI: 10.1103/PhysRevB.72.155412 PACS number(s): 41.20.Cv, 42.25.Fx, 42.68.Mj

I. INTRODUCTION

It is known that nanoscale particles can exhibit resonance behavior at certain frequencies for which the particle permittivity is negative and the free-space wavelength is large in comparison with particle dimensions. The latter condition clearly suggests that these resonances are electrostatic in nature. They appear at specific negative values of the dielectric permittivity for which source-free electrostatic fields may exist. This is, in essence, the physical mechanism of these resonances. For nanoscale metallic particles, these resonances occur in the optical frequency range and they result in powerful localized sources of light that are useful in scanning near-field optical microscopy,[1,2] nanolithography,[3] and in biosensor applications.[4,5] It is also believed[6] that strong local electromagnetic fields associated with these resonances may play an important role in surface enhanced Raman scattering.[7–9] Furthermore, it is anticipated that these resonances may be instrumental in the emerging field of nanophotonics where resonant nanoparticles will be used to guide and switch light at the nanoscale.[10–13] In this way, these resonances may pave the way to all-optical computing where information transmission and processing occur entirely at the optical level. Finally, the utilization of resonant nanoparticles may also dramatically reduce the physical bit size for the next generation of optical data storage disks.[14,15] It is important to stress that electrostatic (plasmon) resonances in metallic colloidal particles are intrinsically nanoscale phenomena, because the two resonance conditions (negative dielectric permittivity and large free-space wavelength in comparison with particle dimensions) can be simultaneously and naturally realized only at the nanoscale.

Resonances in metallic nanoparticles are often found experimentally (or numerically) by using a "trial-and-error" method, i.e., by probing metallic nanoparticles of complex shapes with radiation of various frequencies.[16–19] Direct calculations of resonance values of dielectric permittivity, and the corresponding frequencies of electromagnetic radiations, are clearly preferable. This can be accomplished by formulating the problem of electrostatic (plasmon) resonances as an eigenvalue problem for specific surface integral equations. This was first accomplished by Ouyang and Isaacson[20] and was then extended in subsequent publications.[21–24] The purpose of this paper is the further development of the boundary integral technique for direct calculations of resonance frequencies as well as the analysis of unique physical features of electrostatic resonances. In the paper, the study of strong orthogonality properties of resonance modes is carried out. These orthogonality properties are physically important for the selection of resonance modes that can be coupled to incident electromagnetic radiation. A two-dimensional phenomenon of "twin" spectra and explicit estimates of resonance frequencies in terms of geometrical properties of convex nanoparticles are established. Second-order corrections for resonance values of dielectric permittivities for nanoparticles of arbitrary shapes are derived by employing the boundary integral equation method. The techniques for the tuning of these resonances to desirable frequencies are presented, and electrostatic (plasmon) resonances in semiconductor nanoparticles where these resonances can be controlled through optical manipulation of conduction electron density are discussed. This direction of research is promising for the development of all-optical nanotransistors. As a digression, a plausible plasmon resonance mechanism for

nucleation and formation of ball lightning is outlined. The paper is concluded by the discussion of a numerical technique for the calculation of resonance frequencies and extensive computational results are then presented and compared with known theoretical results and available experimental data.

II. ELECTROSTATIC APPROXIMATION. PLASMON RESONANCES AS AN EIGENVALUE PROBLEM

In our discussion of resonances in metallic nanoparticles we shall follow the traditional approach where all losses are first neglected (as in the case of metallic resonance cavities, for instance) and resonance frequencies are found for lossless systems as frequencies for which source-free electromagnetic fields may exist. In our case, this approach leads to the consideration of resonances in the electrostatic limit where all radiation losses are first neglected. This traditional approach clearly reveals the physical nature of resonances in nanoparticles as electrostatic resonances. It is worthwhile to mention here that in literature these resonances are usually called "plasmons." We believe that the term "electrostatic resonances" is more appropriate. Indeed, since these resonances occur at frequencies for which free-space wavelengths are large in comparison with nanoparticle dimensions, time-harmonic electromagnetic fields within the nanoparticles and around them vary almost with the same phase. As a result, at any instant of time these fields look like electrostatic fields. When the dielectric permittivity of metallic nanoparticles is negative, the uniqueness theorem of electrostatics is not valid. For this reason, source-free electrostatic fields may appear for certain negative values of dielectric permittivities, which is the manifestation of resonances. The frequencies corresponding to the above negative values of permittivity are the resonance frequencies. It is clear from the previous discussion that electrostatic resonances may occur only in particles whose media exhibit dispersion, that is when permittivity is a function of frequency, and its real part assumes negative value for some range of frequencies. For metals, this frequency range is below the plasma frequencies, but at sufficiently high frequencies for collisions to be unimportant. For good conductors such as silver and gold, plasma frequencies are in the visible frequency range, and this explains why silver and gold nanoparticles are usually employed for the observation of electrostatics (plasmon) resonances.

To start the discussion, consider a dielectric object of arbitrary shape with permittivity $\epsilon_+(\omega)$ (Fig. 1). We are interested in negative values of $\epsilon_+(\omega)$ for which a source-free electromagnetic field may exist. To find such permittivities, we shall write Maxwell equations in terms of the vectors

$$\mathbf{e} = \epsilon_0^{1/2}\mathbf{E}, \quad \mathbf{h} = \mu_0^{1/2}\mathbf{H} \tag{1}$$

and spatial coordinates scaled by the diameter d of the object. This leads to the following boundary value problem:

$$\nabla \times \mathbf{e}^+ = -i\beta\mathbf{h}^+, \quad \nabla \times \mathbf{h}^+ = i\frac{\epsilon_+}{\epsilon_0}\beta\mathbf{e}^+, \tag{2}$$

$$\nabla \cdot \mathbf{e}^+ = 0, \quad \nabla \cdot \mathbf{h}^+ = 0, \tag{3}$$

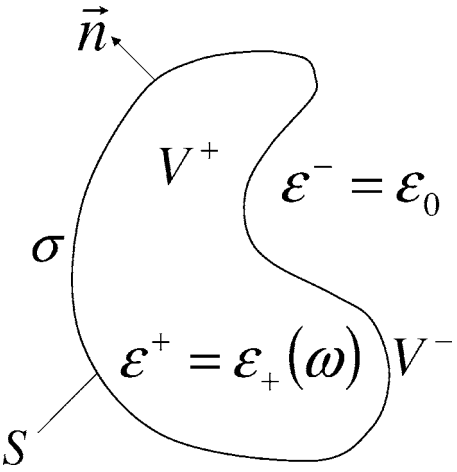

FIG. 1. The dielectric nanoparticle bounded by surface S.

$$\nabla \times \mathbf{e}^- = -i\beta\mathbf{h}^-, \quad \nabla \times \mathbf{h}^- = i\beta\mathbf{e}^-, \tag{4}$$

$$\nabla \cdot \mathbf{e}^- = 0, \quad \nabla \cdot \mathbf{h}^- = 0, \tag{5}$$

$$\mathbf{n} \times (\mathbf{e}^+ - \mathbf{e}^-) = 0, \quad \mathbf{n} \times (\mathbf{h}^+ - \mathbf{h}^-) = 0, \tag{6}$$

$$\mathbf{n} \cdot \left(\frac{\epsilon_+}{\epsilon_0}\mathbf{e}^+ - \mathbf{e}^-\right) = 0, \quad \mathbf{n} \cdot (\mathbf{h}^+ - \mathbf{h}^-) = 0, \tag{7}$$

where superscripts "+" and "−" are used for physical quantities inside (V^+) and outside (V^-) the dielectric object, respectively, $\mathbf{n}$ is a outward unit normal to S, and

$$\beta = \omega\sqrt{\mu_0\epsilon_0}d. \tag{8}$$

In the case when the free-space wavelength is large in comparison with the object dimension, β can be treated as a small parameter and source-free solution of the boundary value problem (2)–(7) and permittivities ϵ_+ at which they occur can be expanded in terms of β:

$$\mathbf{e}^\pm = \mathbf{e}_0^\pm + \beta\mathbf{e}_1^\pm + \beta^2\mathbf{e}_2^\pm + \cdots, \tag{9}$$

$$\mathbf{h}^\pm = \mathbf{h}_0^\pm + \beta\mathbf{h}_1^\pm + \beta^2\mathbf{h}_2^\pm + \cdots, \tag{10}$$

$$\epsilon_+ = \epsilon_+^{(0)} + \beta\epsilon_+^{(1)} + \beta^2\epsilon_+^{(2)} + \cdots. \tag{11}$$

By substituting formulas (9)–(11) into Eqs. (2)–(5) as well as boundary conditions (6) and (7) and equating terms of equal powers of β, we obtain the boundary value problems for $\mathbf{e}_k^\pm$ and $\mathbf{h}_k^\pm$. For zero-order terms, these boundary value problems can be written in terms of $\mathbf{E}_0^\pm = \epsilon_0^{-1/2}\mathbf{e}_0^\pm$ and $\mathbf{H}_0^\pm = \mu_0^{-1/2}\mathbf{h}_0^\pm$ as follows:

$$\nabla \times \mathbf{E}_0^\pm = 0, \quad \nabla \cdot \mathbf{E}_0^\pm = 0, \tag{12}$$

$$\mathbf{n} \times (\mathbf{E}_0^+ - \mathbf{E}_0^-) = 0, \quad \mathbf{n} \cdot \left(\frac{\epsilon_+^{(0)}}{\epsilon_0}\mathbf{E}_0^+ - \mathbf{E}_0^-\right) = 0, \tag{13}$$

and

$$\nabla \times \mathbf{H}_0^\pm = 0, \quad \nabla \cdot \mathbf{H}_0^\pm = 0, \tag{14}$$

$$\mathbf{n} \times (\mathbf{H}_0^+ - \mathbf{H}_0^-) = 0, \quad \mathbf{n} \cdot (\mathbf{H}_0^+ - \mathbf{H}_0^-) = 0. \tag{15}$$

Boundary value problems for higher-order terms as well as high-order corrections for ϵ_+ are discussed in Sec. IV.

It is apparent that

$$\mathbf{H}_0^\pm = 0. \tag{16}$$

The electric potential φ can be introduced for a source-free electric field $\mathbf{E}_0$ and this potential satisfies the following boundary value problem:

$$\nabla^2 \varphi^+ = 0 \quad \text{in } V^+, \quad \nabla^2 \varphi^- = 0 \quad \text{in } V^-, \tag{17}$$

$$\varphi^+ = \varphi^-, \quad \epsilon_+^{(0)} \frac{\partial \varphi^+}{\partial n} = \epsilon_0 \frac{\partial \varphi^-}{\partial n} \quad \text{on } S, \tag{18}$$

and zero boundary conditions at infinity. It is apparent that potential φ can be represented as an electric potential of single layer of electric charges σ distributed over the boundary S of the particle

$$\varphi(Q) = \frac{1}{4\pi\epsilon_0} \oint_S \frac{\sigma(M)}{r_{MQ}} dS_M. \tag{19}$$

In other words, a single layer of electric charges on S may create the same electric field in the free space as the source-free electric field that may exist in the presence of the dielectric particle with negative permittivity. It is clear that this potential satisfies equations (17) and the first boundary condition in Eq. (18). Next, we recall that the normal components of electric field of surface electric charges are given by the formulas[25,26]

$$\mathbf{n}(Q) \cdot \mathbf{E}_0^\pm(Q) = \mp \frac{\sigma(Q)}{2\epsilon_0} + \frac{1}{4\pi\epsilon_0} \oint_S \sigma(M) \frac{\mathbf{r}_{MQ} \cdot \mathbf{n}_Q}{r_{MQ}^3} dS_M. \tag{20}$$

The physical origin of formulas (20) is easy to understand. Indeed, the normal components of electric field are discontinuous across the charged surface because the field created by the elementary surface charge at point Q has opposite directions with respect to the outward normal $\mathbf{n}_Q$. As a result of symmetry, this discontinuity is equally split (for smooth charged surfaces) between the normal components inside and outside S. By substituting formulas (20) into the second boundary condition (13) [or Eq. (18)], after simple transformations we arrive at the following homogeneous boundary integral equation:

$$\sigma(Q) = \frac{\lambda}{2\pi} \oint_S \sigma(M) \frac{\mathbf{r}_{MQ} \cdot \mathbf{n}_Q}{r_{MQ}^3} dS_M, \tag{21}$$

where

$$\lambda = \frac{\epsilon_+^{(0)}(\omega) - \epsilon_0}{\epsilon_+^{(0)}(\omega) + \epsilon_0}. \tag{22}$$

Thus, source-free electric fields may exist only for such values of permittivity $\epsilon_+^{(0)}$ that the integral equation (21) has nonzero solutions. In other words, in order to find the resonance values of $\epsilon_+^{(0)}$ (and the corresponding resonance frequencies) as well as resonance modes, the eigenvalues and eigenfunctions of the integral equation (21) must be computed. The integral equation (21) for the analysis of plasmon resonances was first introduced by Ouyang and Isaacson,[20] while similar inhomogeneous surface integral equations for the calculation of electrostatic and magnetostatic fields as well as scattering problems[23] were previously and extensively used in publications.[27,28]

For particles of complex shapes the resonance frequencies and resonance modes can be found through the numerical solution of integral equation (21). If the boundary S of the particle is not smooth, then $\sigma(M)$ may have singularities at the corners and the edges of S that may negatively affect the accuracy of numerical computations. In this situation, the dual formulation can be employed which is of interest in its own right. In this formulation, the electric displacement field $\mathbf{D}_0$ is introduced instead of electric field $\mathbf{E}_0$. It is easy to see that the potential ϕ for the displacement field ($\mathbf{D}_0 = -\nabla\phi$) is the solution of the following boundary value problem:

$$\nabla^2 \phi^+ = 0 \quad \text{in } V^+, \quad \nabla^2 \phi^- = 0 \quad \text{in } V^-, \tag{23}$$

$$\frac{\partial \phi^+}{\partial n} = \frac{\partial \phi^-}{\partial n}, \quad \frac{\phi^+}{\epsilon^+(\omega)} = \frac{\phi^-}{\epsilon_0} \quad \text{on } S, \tag{24}$$

where zero boundary condition at infinity is tacitly implied.

Potential ϕ can be represented as an electric potential of double layer of electrical charges (dipoles) of density $\tau(M)$ distributed over the boundary S of the particle:

$$\phi(Q) = \frac{1}{4\pi} \oint_S \tau(M) \frac{\mathbf{r}_{QM} \cdot \mathbf{n}_M}{r_{QM}^3} dS_M. \tag{25}$$

In other words, a double layer of electric charges on S may create the same electric displacement field $\mathbf{D}_0$ in free space as the source-free displacement field that may exist in the presence of dielectric particle with negative permittivity. It is clear that double-layer potential (25) satisfies the equations in Eq. (23) and the first boundary condition in Eq. (24). Next, we recall that the boundary values of double-layer potential (25) are given by the formulas[25,26]

$$\phi^\pm(Q) = \pm \frac{\tau(Q)}{2} + \frac{1}{4\pi} \oint_S \tau(M) \frac{\mathbf{r}_{QM} \cdot \mathbf{n}_M}{r_{QM}^3} dS_M. \tag{26}$$

By substituting formulas (26) into the second boundary condition in Eq. (24), after simple transformation we arrive at the following homogeneous boundary integral equation for $\tau(M)$:

$$\tau(Q) = \frac{\lambda}{2\pi} \oint_S \tau(M) \frac{\mathbf{r}_{QM} \cdot \mathbf{n}_M}{r_{QM}^3} dS_M, \tag{27}$$

where λ is given by formula (22). It is apparent that the boundary integral equation (27) is adjoint to the integral equation (21). For this reason, it has the same spectrum (as expected on the physical grounds). The dipole density $\tau(M)$ is proportional to the discontinuity of double-layer potential across S and, consequently, it is finite even for nonsmooth boundaries S. This is the advantage of integral equation (27) for numerical computations with nonsmooth boundaries S.

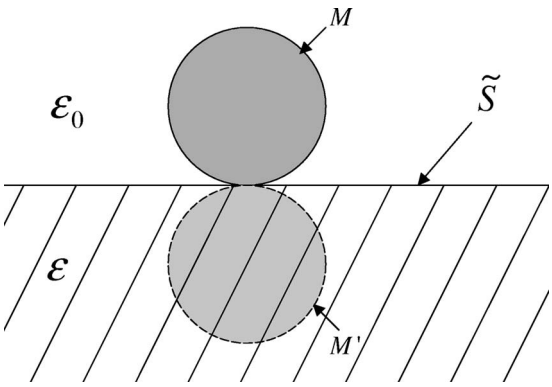

FIG. 2. Nanoparticles on substrate. The "dash particle" is the mirror image of the actual particle on the substrate [see formula (23)].

The presented discussion can be easily extended to the analysis of electrostatic (plasmon) resonances of several particles located in proximity to one another. In this case S in integral equations (21) and (27) must be construed as the union of boundaries of all dielectric particles, while $\sigma(M)$ [and $\tau(M)$] are defined on this union.

In applications, nanoparticles are located on dielectric substrates (see Fig. 2). In this case, the integral equation (21) can be modified as follows:

$$\sigma(Q) = \frac{\lambda}{2\pi} \oint_S \sigma(M)\mathbf{n}(Q) \cdot \nabla_Q [G(Q,M)] dS_M, \qquad (28)$$

where λ is given by formula (22), while $G(M,Q)$ is the Green function defined by the formula

$$G(Q,M) = \frac{1}{r_{MQ}} - \frac{\epsilon - \epsilon_0}{\epsilon + \epsilon_0} \frac{1}{r_{M'Q}}. \qquad (29)$$

Here, ϵ is the permittivity of the substrate and M' is the image of M with respect to the substrate plane $\tilde{S}$.

It is worthwhile to mention that there exists in literature[29,30] another eigenvalue-type approach to plasmon resonance analysis in which the boundary value problem (17) and (18) is simply construed as a generalized differential eigenvalue problem. From the computational point of view, the eigenvalue approach based on integral equations (21) and (27) is more efficient. Indeed, discretizations of surface integral equations (21) and (27) result in the classical (standard) matrix eigenvalue problem, which is not the case for the generalized differential eigenvalue problem. In addition, well-known difficulties appear in discretization of the boundary value problem (17) and (18) in the entire space, while no such difficulties encountered in discretizations of surface integral equations (21) and (27).

III. GENERAL PROPERTIES OF RESONANCES

The kernels in integral equations (21), (27), and (28) have weak (integrable in the usual sense) singularities. For this reason, the integral operators in the above integral equations are compact. This implies that the plasmon spectrum is discrete despite the infinite region of field distribution.

It has been demonstrated[25,26] that the spectrum of integral equation (21) has the following properties: for any shape of S all eigenvalues are real, $\lambda = 1$ is an eigenvalue, and for all other eigenvalues $|\lambda| > 1$. It is apparent from Eq. (22) that the eigenvalue $\lambda = 1$ corresponds to the case of $\epsilon_+^{(0)} \to \infty$, and the respective eigenfunction $\sigma(M)$ can be construed as the distribution of surface electric charges over the boundary S of a conductor V^+. This eigenvalue is irrelevant as far as the discussion of electrostatic (plasmon) resonances is concerned. All other eigenvalues correspond to source-free (resonance) configurations of electrostatic fields and, according to Eq. (22), these configurations may exist (as expected) only for negative values of $\epsilon_+^{(0)}$. After these negative resonance values of $\epsilon_+^{(0)}$ are found through the solution of integral equation (21), the appropriate dispersion relation can be employed to find the corresponding resonance frequencies. When losses are not neglected, actual permittivities are complex-valued functions of frequency ω. These permittivities may assume real resonance values $\epsilon_+^{(0)}$ only for complex resonance frequencies.

It is instructive to note that the "plasmon" eigenfunctions of integral equation (21) have the property

$$\oint_S \sigma(M) dS_M = 0. \qquad (30)$$

Indeed, by integrating both sides of Eq. (21) with respect to Q and by using the facts that

$$\oint_S \frac{\mathbf{r}_{MQ} \cdot \mathbf{n}_Q}{r_{MQ}^3} dS_Q = 2\pi \qquad (31)$$

and $\lambda \neq 1$ for plasmon resonances, we arrive at Eq. (30).

It is apparent that the mathematical structure of integral equation (21) is invariant with respect to the scaling of S, i.e., the scaling of the dimensions of the particle. This leads to the unique property of electrostatic (plasmon) resonances: resonance frequencies depend on particle shape but they are scale invariant with respect to particle dimensions, provided that they remain appreciably smaller than the free-space wavelength.

A. Strong orthogonality of plasmon modes and excitation conditions

The integral operator in Eq. (21) is not Hermitian (not self-adjoint), because the kernel of this equation is not symmetric. For this reason, the eigenfunctions $\sigma_i(M)$ and $\sigma_k(M)$ corresponding to different eigenvalues λ_i and λ_k are not orthogonal on S in the usual sense. Nevertheless, it can be shown that electric fields $\mathbf{E}_{0i}$ and $\mathbf{E}_{0k}$ corresponding to eigenfunctions $\sigma_i(M)$ and $\sigma_k(M)$ satisfy the following strong orthogonality conditions:

$$\int_{V^\pm} \mathbf{E}_{0i} \cdot \mathbf{E}_{0k} dV = 0. \qquad (32)$$

The peculiar feature of the above strong orthogonality conditions is that they hold separately in regions V^+ and V^-. The

orthogonality conditions of eigenfunctions in the entire space was previously found in Refs. 20 and 30. The proof of the above strong orthogonality conditions proceeds as follows. By using formulas (20), the integral equation (21) for the eigenfunction $\sigma_k(M)$ can be written in the form

$$\mathbf{n}\cdot(\mathbf{E}_{0k}^{-}-\mathbf{E}_{0k}^{+})=\lambda_k\mathbf{n}\cdot(\mathbf{E}_{0k}^{-}+\mathbf{E}_{0k}^{+}). \tag{33}$$

By multiplying both sides of formula (33) by electric potential φ_i created by charges $\sigma_i(M)$ and integrating over S, we obtain

$$(\lambda_k-1)\oint_S \varphi_i\mathbf{E}_{0k}^{-}\cdot\mathbf{n}dS=-(\lambda_k+1)\oint_S \varphi_i\mathbf{E}_{0k}^{+}\cdot\mathbf{n}dS. \tag{34}$$

Now, by using the divergence theorem and the facts that $\nabla\cdot\mathbf{E}_{0k}^{\pm}=0$ and $\mathbf{E}_{0i}=-\nabla\varphi_i$, we arrive at

$$(\lambda_k-1)\int_{V^-}\mathbf{E}_{0i}^{-}\cdot\mathbf{E}_{0k}^{-}dV=(\lambda_k+1)\int_{V^+}\mathbf{E}_{0i}^{+}\cdot\mathbf{E}_{0k}^{+}dV. \tag{35}$$

By considering the integral equation (21) for the eigenfunction $\sigma_i(M)$ and by repeating the same line of reasoning as in the derivation of formula (34), we arrive at

$$(\lambda_i-1)\int_{V^-}\mathbf{E}_{0k}^{-}\cdot\mathbf{E}_{0i}^{-}dV=(\lambda_i+1)\int_{V^+}\mathbf{E}_{0k}^{+}\cdot\mathbf{E}_{0i}^{+}dV. \tag{36}$$

Since $\lambda_k\neq\lambda_i$, the orthogonality conditions (32) follow from formulas (35) and (36).

The orthogonality conditions (32) can be instrumental in the analysis of the coupling of a specific resonance mode to incident electromagnetic fields. Indeed, by expanding the incident field in V^+ into series with respect to resonance modes $\mathbf{E}_{0k}^{+}$, it can be shown that only resonance modes with nonzero expansion coefficients can be coupled to the incident radiation. The demonstration proceeds as follows. First, it can be remarked that eigenfunctions $\sigma_i(M)$ and $\tau_i(M)$ of adjoint equations (21) and (27) form two biorthogonal sets

$$\langle\sigma_k,\tau_j\rangle=\oint_S\sigma_k(M)\tau_j(M)dS_M=\delta_{kj}, \tag{37}$$

where δ_{kj} is the Kronecker delta. Then, it is easy to see that in the presence of an incident field $\mathbf{E}^{(i)}$, Eq. (21) is modified as follows:

$$\sigma(Q)-\frac{\lambda}{2\pi}\oint_S\sigma(M)\frac{\mathbf{r}_{MQ}\cdot\mathbf{n}_Q}{r_{MQ}^3}dS_M=2\epsilon_0\lambda\mathbf{n}\cdot\mathbf{E}^{(i)}(Q). \tag{38}$$

Next, by expanding $\sigma(Q)$ and $\mathbf{n}\cdot\mathbf{E}^{(i)}(Q)$ in terms of σ_k and by using formulas (21) and (37), we derive the following expression for the solution of integral equation (38):

$$\sigma(Q)=2\epsilon_0\lambda\sum_k\frac{\lambda_k}{\lambda_k-\lambda}\langle\mathbf{n}\cdot\mathbf{E}^{(i)},\tau_k\rangle\sigma_k(Q). \tag{39}$$

It is clear from Eq. (39) that the solution of integral equation (38) blows up as λ approaches λ_k, which is the manifestation of electrostatic (plasmon) resonances at the frequencies corresponding to λ_k. It is also apparent that these resonances occur only if

$$\langle\mathbf{n}\cdot\mathbf{E}^{(i)},\tau_k\rangle=\oint_S\tau_k(M)\mathbf{n}_M\cdot\mathbf{E}^{(i)}(M)dS_M\neq 0. \tag{40}$$

It can be inferred that $\tau_k(M)$ is proportional to the potential $\varphi_k^{+}(M)$ of the corresponding resonance mode on S. Consequently,

$$\langle\mathbf{n}\cdot\mathbf{E}^{(i)},\tau_k\rangle=\alpha\oint_S\varphi_k^{+}(M)\mathbf{n}_M\cdot\mathbf{E}^{(i)}(M)dS_M=-\alpha\int_{V^+}\mathbf{E}_{0k}^{+}(M)\cdot\mathbf{E}^{(i)}(M)dV_M. \tag{41}$$

By using formulas (39) and (41), it can be concluded that only plasmon resonance modes with nonzero coefficients in the expansion of $\mathbf{E}^{(i)}$ in V^+ with respect to $\mathbf{E}_{0k}^{+}$ can be coupled to the incident radiation. If the incident field is uniform in V^+, then only resonance modes with nonzero average values of electric field components over V^+ have nonzero expansion coefficients and can be effectively excited. For instance, it will be demonstrated below that for a sphere and for ellipsoids there are resonance modes with uniform electric fields in V^+. This means that according to the strong orthogonality condition in V^+ only these "uniform" resonance modes will be excited by uniform (within V^+) incident radiation. The condition of uniformity within V^+ of the incident radiation is quite natural due to the smallness of particle dimensions in comparison with the free-space wavelength of the incident radiation. For particles of complex shapes, many resonance modes with appreciable average values of electric field components over V^+ may exist. All such modes will be well coupled to the uniform incident radiation and can be excited by such incident fields at the respective resonance frequencies.

It can be shown that the average electric field over V^+ is proportional to the total electric dipole moment as computed by using either the surface charge distribution σ or the double layer density τ. Indeed, the x-component of electric dipole moment can be expressed in terms of σ_k as follows:

$$p_x^{(k)}=\oint_S x\sigma_k dS. \tag{42}$$

It is apparent that σ is proportional to $\mathbf{n}\cdot\mathbf{E}_{0k}^{+}$. Consequently,

$$p_x^{(k)}=\alpha\oint_S x\mathbf{n}\cdot\mathbf{E}_{0k}^{+}dS=\alpha\int_{V^+}E_{x0k}^{+}dV, \tag{43}$$

which implies that

$$\mathbf{p}^{(k)}=\alpha\int_{V^+}\mathbf{E}_{0k}^{+}dV. \tag{44}$$

Similarly,

$$p_x^{(k)} = \alpha \oint_S \tau_k \mathbf{a}_x \cdot \mathbf{n} dS, \tag{45}$$

where $\mathbf{a}_x$ is a unit vector along the x axis. But τ_k is proportional to φ_k^+. Consequently,

$$p_x^{(k)} = \alpha \oint_S \varphi_k^+ \mathbf{a}_x \cdot \mathbf{n} dS = -\alpha \int_{V^+} E_{x0k}^+ dV. \tag{46}$$

Finally, we remark that the modes with a non-zero dipole moment not only couple to a uniform applied field but also are effective radiators of electromagnetic waves.

B. Twin spectra in two dimensions

For two-dimensional objects (i.e., nanowires), the integral equation (21) is modified as follows:

$$\sigma(Q) = \frac{\lambda}{\pi} \oint_S \sigma(M) \frac{\mathbf{r}_{MQ} \cdot \mathbf{n}_Q}{r_{MQ}^2} dS_M, \tag{47}$$

where S is now the boundary curve with line element dS, and the potential is the logarithmic potential created by the line charge with density σ.

It turns out that for two-dimensional problems an interesting phenomena of twin spectra occurs where for any cross-section shape (any S) the set of eigenvalues consists of positive λ_n^+ and negative λ_n^- numbers such that

$$\lambda_n^+ = -\lambda_n^-. \tag{48}$$

The origin of twin spectrum can be traced to the fact that for two-dimensional problems the stream function ψ for vector field $\mathbf{D}$ can be introduced: $\mathbf{D} = \mathbf{a} \times \nabla \psi$, where $\mathbf{a}$ is the unit vector normal to cross-sectional planes. Due to the property (30), the stream function is single valued. It is apparent that this stream function is a solution of the following boundary value problem:

$$\nabla^2 \psi^+ = 0 \quad \text{in } V^+, \quad \nabla^2 \psi^- = 0 \quad \text{in } V^-, \tag{49}$$

$$\psi^+ = \psi^-, \quad \frac{1}{\epsilon_+^{(0)}} \frac{\partial \psi^+}{\partial n} = \frac{1}{\epsilon_0} \frac{\partial \psi^-}{\partial n} \quad \text{on } S. \tag{50}$$

This boundary value problem coincides with the boundary value problem (17) and (18) for electric potential, when $\epsilon_+^{(0)}$ is replaced by $\epsilon_0^2/\epsilon_+^{(0)}$. This implies that electrostatic (plasmon) resonances simultaneously exist for reciprocal values of relative dielectric permittivity. By using this fact and formula (22), we arrive at the twin spectrum relation (48). As an illustration, we mention that in the case of elliptic nanowires, the following expression for the twin spectrum can be analytically derived:

$$\lambda_n^{\pm} = \pm \left(\frac{a+b}{a-b} \right)^n, \tag{51}$$

where a and b are major and minor axes, respectively.

C. Eigenvalue estimates

For three-dimensional problems with convex boundary S, the following estimate for eigenvalues λ can be derived:

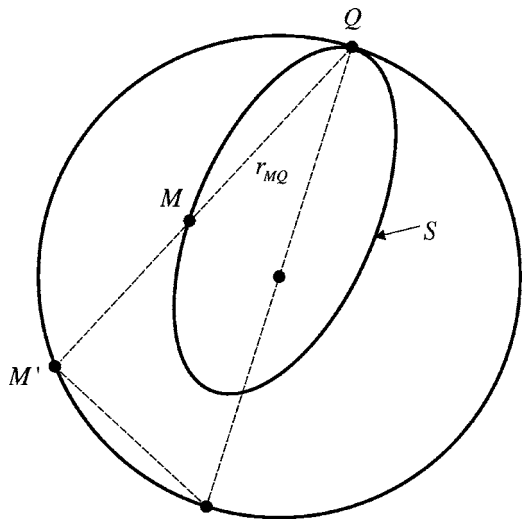

FIG. 3. Geometric illustration of Blaschke's theorem.

$$|\lambda| > c = \frac{1}{1 - \dfrac{A}{4\pi R d}}, \tag{52}$$

where A is the area of S, R is the maximum radius of the curvature of S, and d is the diameter of V^+. The derivation of inequality (52) is based on the fact that for convex S the kernel of integral equation (21) is positive and the following estimate is valid:

$$\frac{\mathbf{r}_{MQ} \cdot \mathbf{n}_Q}{r_{MQ}^3} > \frac{1}{2Rd}. \tag{53}$$

Indeed, according to the Blaschke theorem[31] for any point Q the surface S is contained inside the sphere of radius R tangential to S at Q (Fig. 3). Consequently,

$$\frac{\mathbf{r}_{MQ} \cdot \mathbf{n}_Q}{r_{MQ}^3} = \frac{\cos \gamma}{r_{MQ}^2} \geqslant \frac{\cos \gamma}{r_{M'Q} \cdot r_{MQ}} > \frac{1}{2Rd}. \tag{54}$$

Now, the proof (52) proceeds as follows. According to the property (30), we find

$$\int_{S_\sigma^+} \sigma(Q) dS_Q = \int_{S_\sigma^-} |\sigma(Q)| dS_Q = \frac{1}{2} \oint_S |\sigma(Q)| dS_Q, \tag{55}$$

where S_σ^+ and S_σ^- are the parts of S for which $\sigma(Q)$ is positive and negative, respectively.

Consider first the case when $\lambda > 0$. Then from integral equations (21) and (55) we obtain

$$\oint_S |\sigma(Q)| dS_Q = 2 \int_{S_\sigma^+} \sigma(Q) dS_Q = \frac{\lambda}{\pi} \oint_S \sigma(M) \left(\int_{S_\sigma^+} \frac{\mathbf{r}_{MQ} \cdot \mathbf{n}_Q}{r_{MQ}^3} dS_Q \right) dS_M, \tag{56}$$

where the last double integral is strictly positive. Next, by using formulas (31), (53), (55), and (56), we derive:

$$\oint_S |\sigma(Q)|dS_Q = \frac{\lambda}{\pi}\Bigg[2\pi\int_{S_\sigma^+}\sigma(M)dS_M - \int_{S_\sigma^+}\sigma(M)\left(\int_{S_\sigma^-}\frac{\mathbf{r}_{MQ}\cdot\mathbf{n}_Q}{r_{MQ}^3}dS_Q\right)dS_M - \int_{S_\sigma^-}|\sigma(M)|\left(\int_{S_\sigma^+}\frac{\mathbf{r}_{MQ}\cdot\mathbf{n}_Q}{r_{MQ}^3}dS_Q\right)dS_M\Bigg] < \lambda\left(1-\frac{A}{4\pi Rd}\right)\oint_S|\sigma(M)|dS_M. \quad (57)$$

From the last inequality follows

$$\lambda > \frac{1}{1-\frac{A}{4\pi Rd}}. \quad (58)$$

In the case $\lambda<0$, from integral equation (21) and formula (55) we obtain

$$\oint_S |\sigma(Q)|dS_Q = -2\int_{S_\sigma^-}\sigma(Q)dS_Q = -\frac{\lambda}{\pi}\oint_S\sigma(M)\left(\int_{S_\sigma^-}\frac{\mathbf{r}_{MQ}\cdot\mathbf{n}_Q}{r_{MQ}^3}dS_Q\right)dS_M. \quad (59)$$

Now, by using the same line of reasoning as in the derivation of Eq. (58), we arrive at the inequality

$$\lambda < -\frac{1}{1-\frac{A}{4\pi Rd}}, \quad (60)$$

which together with Eq. (58) is tantamount to inequality (52). By using inequality (52) and formula (22), the following upper and lower bounds for possible resonance values of permittivity $\epsilon_+^{(0)}(\omega)$ can be obtained:

$$\frac{1+c}{1-c} < \frac{\epsilon_+^{(0)}(\omega)}{\epsilon_0} < \frac{1-c}{1+c}. \quad (61)$$

For the common dispersion relation

$$\epsilon_+^{(0)}(\omega) = \epsilon_0\left(1-\frac{\omega_p^2}{\omega^2}\right), \quad (62)$$

the previous formula leads to the following upper and lower bounds for resonance frequencies

$$\frac{c-1}{2c} < \frac{\omega^2}{\omega_p^2} < \frac{c+1}{2c}, \quad (63)$$

which suggests that the bandwidth for resonance frequencies is smaller than $\omega_p/\sqrt{c}=\omega_p\sqrt{1-A/4\pi Rd}$.

In the case of nanowires with convex boundaries, it can be shown by using the same line of reasoning as before that the following inequality for eigenvalues of integral equation (47) is valid:

$$|\lambda| \geqslant \frac{1}{1-\frac{L}{2\pi R}}, \quad (64)$$

where L is the length of the cross-sectional boundary, while R is the maximum radius of its curvature. The last inequality is isoperimetric in a sense that it is exact for nanowires of circular cross sections for which electrostatic (plasmon) resonances occur only for $\epsilon_+^{(0)}(\omega)=-\epsilon_0$ which corresponds to $\lambda=\infty$.

D. Symmetry and spectrum

In the case when the boundary S is symmetric, certain qualitative features of the electrostatic (plasmon) spectrum can be predicted by using irreducible representations of the symmetry group of the boundary S. For instance, the multiplicities of eigenvalues λ of integral equation (21) are equal to the dimensions of inequivalent irreducible representations of the symmetry group of the boundary S. By using the irreducible representations of the symmetry groups, selection rules for plasmon modes with zero dipole moment can be constructed. These plasmon modes cannot be excited by uniform (in V^+) incident radiation. These rules can be explained as follows. The dipole moment is a vector, and transforms accordingly under rotations and reflections, so that it generates a representation of the symmetry group. This representation can be decomposed into a direct sum of irreducible representations. Then only modes that are transformed by these particular irreducible representations can have a nonzero dipole moment.

Consider as an example a nanowire whose cross section is an equilateral triangle. This triangle is invariant with respect to the transformations of the group C_{3v}.[32] This group has three inequivalent irreducible representations: two of dimension one and one of dimension two. This fact implies that the spectrum is likely to consist only of simple and twofold degenerate eigenvalues. It can also be shown that the dipole moments of resonance modes corresponding to simple eigenvalues are equal to zero. This group theory prediction is consistent with our numerical results obtained through numerical solution of integral equation (47) and shown in Table I.

As another example, consider a spherical particle of unit radius. In this case the kernel of integral equation (21) is equal to $1/2r_{MQ}$. By using this fact, it is easy to demonstrate that the spherical harmonics $Y_{lm}(\theta,\varphi)$ are the eigenfunctions corresponding to the eigenvalue $\lambda_l=2l+1$. According to Eq. (22), the corresponding resonance values of permittivity are $\epsilon_{+l}^{(0)}=-\epsilon_0(1+1/l)$. Because of the scale invariance of eigenvalues λ_l, the same $\epsilon_{+l}^{(0)}$ are the resonance permittivity values for a spherical nanoparticle of arbitrary radius provided that the latter is much smaller than the free-space wavelength of incident radiation. These resonance permittivity values are consistent with the classical Mie theory.[33] The three lowest electrostatic (plasmon) modes are uniform in V^+ and only these modes can be excited by uniform (within V^+) incident radiation. It is apparent that the multiplicities of eigenvalues λ_l are equal to $2l+1$ and they coincide with the dimensions

TABLE I. Numerical results for the equilateral triangle.

Eigenvalues (λ)	p_x	p_y
1.0015	0.0000	0.0000
−2.4459	−0.1681	−0.3028
−2.4459	−0.3094	0.1556
2.4649	−0.0472	−0.6230
2.4649	−0.6244	0.0200
−4.3263	−0.0000	−0.0000
4.3809	−0.0000	−0.0000
−13.3646	−0.0421	0.0656
−13.3646	0.0628	0.0461
13.5374	−0.0267	0.0808
13.5374	0.0149	−0.0838

of irreducible representations of the rotation group, which is the symmetry group of the sphere.

IV. FIRST- AND SECOND-ORDER CORRECTIONS

From formulas (2)–(7), (9)–(11), and (16), we derive the following boundary value problems for the first-order corrections $\mathbf{e}_1^{\pm}$, $\epsilon_+^{(1)}$, and $\mathbf{h}_1^{\pm}$, respectively:

$$\nabla \times \mathbf{e}_1^{\pm} = 0, \quad \nabla \cdot \mathbf{e}_1^{\pm} = 0, \tag{65}$$

$$\mathbf{n} \times (\mathbf{e}_1^{+} - \mathbf{e}_1^{-}) = 0, \quad \mathbf{n} \cdot \left(\frac{\epsilon_+^{(0)}}{\epsilon_0} \mathbf{e}_1^{+} - \mathbf{e}_1^{-} \right) = - \frac{\epsilon_+^{(1)}}{\epsilon_0} \mathbf{n} \cdot \mathbf{e}_0^{+} \tag{66}$$

and

$$\nabla \times \mathbf{h}_1^{+} = i \frac{\epsilon_+^{(0)}}{\epsilon_0} \mathbf{e}_0^{+}, \quad \nabla \times \mathbf{h}_1^{-} = i \mathbf{e}_0^{-}, \quad \nabla \cdot \mathbf{h}_1^{\pm} = 0, \tag{67}$$

$$\mathbf{n} \times (\mathbf{h}_1^{+} - \mathbf{h}_1^{-}) = 0, \quad \mathbf{n} \cdot (\mathbf{h}_1^{+} - \mathbf{h}_1^{-}) = 0, \tag{68}$$

where as before $\mathbf{e}_0^{\pm} = \epsilon_0^{1/2} \mathbf{E}_0^{\pm}$.

The electric potential φ_1 of single layer of electric charges σ_1 distributed over S can be introduced for the electric field $\mathbf{e}_1^{\pm}$ [see formula (19)]. Then, by using formulas (20) and the same reasoning as in the derivation of integral equation (21), we arrive at the following integral equation for $\sigma_1(M)$:

$$\sigma_1(Q) - \frac{\lambda}{2\pi} \oint_S \sigma_1(M) \frac{\mathbf{r}_{MQ} \cdot \mathbf{n}_Q}{r_{MQ}^3} dS_M = \epsilon_+^{(1)} \frac{2\epsilon_0}{\epsilon_+^{(0)} + \epsilon_0} \mathbf{n}_Q \cdot \mathbf{e}_0^{+}(Q), \tag{69}$$

where λ is given by formula (22).

It is clear that λ is one of the eigenvalues of integral equation (21), because only for such λ nonzero field $\mathbf{e}_0$ exists. Since λ in Eq. (69) is an eigenvalue, a solution to Eq. (69) exists only under the condition that the right-hand side of Eq. (69) is orthogonal on S to a nonzero solution $\tau(Q)$ of the corresponding homogeneous adjoint equation (27) with the same eigenvalue λ (this is the so-called "normal solvability condition"). It is clear that $\mathbf{n}_Q \cdot \mathbf{e}_0^{+}(Q)$ is proportional to $(\partial \varphi^{+} / \partial n)(Q)$. By using the well-known properties of double-layer potential,[25,26] it can be shown that $\tau(Q)$ is proportional to $\varphi^{+}(Q)$. Consequently,

$$\oint_S \tau(Q) \mathbf{n}_Q \cdot \mathbf{e}_0^{+} dS_Q = \alpha \oint_S \varphi^{+}(Q) \frac{\partial \varphi^{+}}{\partial n}(Q) dS_Q = \alpha \oint_{V^{+}} |\nabla \varphi^{+}|^2 dV \neq 0. \tag{70}$$

This means that the integral equation (69) is only solvable if

$$\epsilon_+^{(1)} = 0. \tag{71}$$

Thus, for any shape of nanoparticles the first order correction for resonant values of dielectric permittivity is equal to zero. As a result of Eq. (71), integral equation (69) is reduced to a homogeneous integral equation identical to Eq. (21). This implies that up to a scale $\sigma(M)$ and $\sigma_1(M)$ as well as $\mathbf{e}_0^{\pm}$ and $\mathbf{e}_1^{\pm}$ are identical. For this reason, it can be assumed that

$$\mathbf{e}_1^{\pm} = 0. \tag{72}$$

Next, we proceed to the solution of boundary value problem (67) and (68). Terms $i(\epsilon_+^{(0)}/\epsilon_0)\mathbf{e}_0^{+}$ and $i\mathbf{e}_0^{-}$ in the first two equations (67) can be interpreted as current sources and the solution of boundary value problem (67) and (68) can be written in the following integral form:

$$\mathbf{h}_1(Q) = \frac{i\epsilon_+^{(0)}}{4\pi\epsilon_0} \int_{V^{+}} \frac{\mathbf{e}_0^{+}(M) \times \mathbf{r}_{MQ}}{r_{MQ}^3} dV_M + \frac{i}{4\pi} \int_{V^{-}} \frac{\mathbf{e}_0^{-}(M) \times \mathbf{r}_{MQ}}{r_{MQ}^3} dV_M. \tag{73}$$

The last expression can be appreciably simplified and reduced to an integral over the boundary S. Indeed, by using the fact that $\nabla \times \mathbf{e}_0^{\pm} = 0$ and by employing the "curl theorem,"[34] after simple transformations we arrive at

$$\mathbf{h}_1(Q) = - \frac{i\left(\frac{\epsilon_+^{(0)}}{\epsilon_0} - 1 \right)}{4\pi} \oint_S \frac{\mathbf{n}_M \times \mathbf{e}_0(M)}{r_{MQ}} dS_M. \tag{74}$$

Now, we proceed to the discussion of second order corrections for $\epsilon_+(\omega)$. From formulas (2)–(7), (9)–(11), (71), and (72) we derive the following boundary value problems for the second-order corrections $\mathbf{e}_2^{\pm}$, $\epsilon_+^{(2)}$, and $\mathbf{h}_2^{\pm}$, respectively:

$$\nabla \times \mathbf{e}_2^{\pm} = - i \mathbf{h}_1^{\pm}, \quad \nabla \cdot \mathbf{e}_2^{\pm} = 0, \tag{75}$$

$$\mathbf{n} \times (\mathbf{e}_2^{+} - \mathbf{e}_2^{-}) = 0, \quad \mathbf{n} \cdot \left(\frac{\epsilon_+^{(0)}}{\epsilon_0} \mathbf{e}_2^{+} - \mathbf{e}_2^{-} \right) = - \frac{\epsilon_+^{(2)}}{\epsilon_0} \mathbf{n} \cdot \mathbf{e}_0^{+} \tag{76}$$

and

$$\nabla \times \mathbf{h}_2^{\pm} = 0, \quad \nabla \cdot \mathbf{h}_2^{\pm} = 0, \tag{77}$$

$$\mathbf{n}\times(\mathbf{h}_2^+-\mathbf{h}_2^-)=0,\quad \mathbf{n}\cdot(\mathbf{h}_2^+-\mathbf{h}_2^-)=0, \tag{78}$$

It is apparent from Eqs. (77) and (78) that

$$\mathbf{h}_2^\pm=0. \tag{79}$$

We shall split the electric field $\mathbf{e}_2^\pm$ into two components

$$\mathbf{e}_2^\pm=\tilde{\mathbf{e}}_2^\pm+\tilde{\tilde{\mathbf{e}}}_2^\pm, \tag{80}$$

that satisfy the following boundary value problems, respectively:

$$\nabla\times\tilde{\mathbf{e}}_2=-i\mathbf{h}_1,\quad \nabla\cdot\tilde{\mathbf{e}}_2=0, \tag{81}$$

$$\mathbf{n}\times(\tilde{\mathbf{e}}_2^+-\tilde{\mathbf{e}}_2^-)=0,\quad \mathbf{n}\cdot(\tilde{\mathbf{e}}_2^+-\tilde{\mathbf{e}}_2^-)=0 \tag{82}$$

and

$$\nabla\times\tilde{\tilde{\mathbf{e}}}_2^\pm=0,\quad \nabla\cdot\tilde{\tilde{\mathbf{e}}}_2^\pm=0, \tag{83}$$

$$\mathbf{n}\times(\tilde{\tilde{\mathbf{e}}}_2^+-\tilde{\tilde{\mathbf{e}}}_2^-)=0,$$

$$\mathbf{n}\cdot\left(\frac{\epsilon_+^{(0)}}{\epsilon_0}\tilde{\tilde{\mathbf{e}}}_2^+-\tilde{\tilde{\mathbf{e}}}_2^-\right)=-\mathbf{n}\cdot\left[\frac{\epsilon_+^{(2)}}{\epsilon_0}\mathbf{e}_0^+ +\left(\frac{\epsilon_+^{(0)}}{\epsilon_0}-1\right)\tilde{\mathbf{e}}_2^+\right]. \tag{84}$$

The solution of the boundary value problem (81) and (82) is

$$\tilde{\mathbf{e}}_2(P)=-\frac{i}{4\pi}\int_{R^3}\frac{\mathbf{h}_1(Q)\times\mathbf{r}_{QP}}{r_{QP}^3}dV_Q. \tag{85}$$

By substituting the expression (74) into the last formula and by changing the order of integration, we arrive at

$$\tilde{\mathbf{e}}_2(P)=-\frac{\left(\frac{\epsilon_+^{(0)}}{\epsilon_0}-1\right)}{16\pi^2}\oint_S[\mathbf{n}_M\times\mathbf{e}_0(M)]\times\left(\int_{R^3}\frac{\mathbf{r}_{QP}}{r_{QP}^3}\frac{1}{r_{QM}}dV_Q\right)dS_M. \tag{86}$$

Consider the following vector function:

$$\mathbf{a}(P,M)=\frac{1}{4\pi\epsilon_0}\int_{R^3}\frac{\mathbf{r}_{QP}}{r_{QP}^3}\frac{1}{r_{QM}}dV_Q. \tag{87}$$

It can be construed as an electric field at point P created by electric charges of volume density $1/r_{QM}$. If we choose point M as the coordinate origin, then this electric field is spherically symmetric and $\mathbf{a}(P,M)$ can be computed by using the Gauss law. The final result is given by the formula

$$\mathbf{a}(P,M)=\frac{\mathbf{r}_{MP}}{2\epsilon_0 r_{MP}}, \tag{88}$$

which implies that

$$\int_{R^3}\frac{\mathbf{r}_{QP}}{r_{QP}^3}\frac{1}{r_{QM}}dV_Q=2\pi\frac{\mathbf{r}_{MP}}{r_{MP}}. \tag{89}$$

By substituting the last expression into formula (86), we end up with

$$\tilde{\mathbf{e}}_2(P)=-\frac{\left(\frac{\epsilon_+^{(0)}}{\epsilon_0}-1\right)}{8\pi}\oint_S\frac{[\mathbf{n}_M\times\mathbf{e}_0(M)]\times\mathbf{r}_{MP}}{r_{MP}}dS_M. \tag{90}$$

Next, we proceed to the solution of the boundary value problem (83) and (84). It is apparent that the electric potential φ_2 of single layer of electric charges $\sigma_2(M)$ distributed over S can be introduced for the electric field $\tilde{\tilde{\mathbf{e}}}_2^\pm$. Then, by using formulas (20) and the same line of reasoning as in the derivation of integral equation (21), we obtain the following integral equation for $\sigma_2(M)$:

$$\sigma_2(Q)-\frac{\lambda}{2\pi}\oint_S\sigma_2(M)\frac{\mathbf{r}_{MQ}\cdot\mathbf{n}_Q}{r_{MQ}^3}dS_M=\frac{2\epsilon_0^2}{\epsilon_0-\epsilon_+^{(0)}}\mathbf{n}\cdot\left[\frac{\epsilon_+^{(2)}}{\epsilon_0}\mathbf{e}_0^+ +\left(\frac{\epsilon_+^{(0)}}{\epsilon_0}-1\right)\tilde{\mathbf{e}}_2^+\right], \tag{91}$$

where as before λ is given by formula (22) and is one of the eigenvalues of integral equation (21). Since λ is an eigenvalue, a solution to Eq. (91) exists only under the condition that the right-hand side of Eq. (91) is orthogonal on S to a nonzero solution $\tau(Q)$ of the corresponding homogeneous adjoint equation (27). This normal solvability condition leads to the following expression for the second order correction $\epsilon_+^{(2)}$ of resonant permittivity:

$$\epsilon_+^{(2)}=-\frac{\epsilon_0\left(\frac{\epsilon_+^{(0)}}{\epsilon_0}-1\right)\oint_S\tau(Q)\mathbf{n}_Q\cdot\tilde{\mathbf{e}}_2^+(Q)dS_Q}{\oint_S\tau(Q)\mathbf{n}_Q\cdot\mathbf{e}_0^+(Q)dS_Q}. \tag{92}$$

Thus, the algorithm for computation of the second order correction $\epsilon_+^{(2)}$ can be stated as follows: first, integral equations (21) and (27) are solved and for each eigenvalue the corresponding $\epsilon_+^{(0)}$ and eigenfunction $\sigma(M)$ and $\tau(M)$ are found; then, by using formula (90), $\tilde{\mathbf{e}}_2^+$ is computed on S; finally, by employing expression (92), the second-order corrections $\epsilon_+^{(2)}$ to resonant permittivities $\epsilon_+^{(0)}$ can be calculated. According to Eqs. (11) and (71), the resonant permittivities are given by the formula

$$\epsilon_+=\epsilon_+^{(0)}+\beta^2\epsilon_+^{(2)}, \tag{93}$$

where β is defined in Eq. (8).

The computations outlined above can be performed analytically in the case of spherical nanoparticles. They are straightforward but lengthy. The final result for the first three (spatially uniform) modes is

$$\epsilon_+=-\left(2+\frac{3}{5}\beta^2\right)\epsilon_0=-\left(2+\frac{12}{5}\omega^2\mu_0\epsilon_0 a^2\right)\epsilon_0, \tag{94}$$

where a is the radius of spherical nanoparticle. The result (94) is the same as obtained from the Mie theory.[33]

V. TUNABILITY AND CONTROLLABILITY OF RESONANCES

It is of interest to design nanoparticles that will resonate at specified frequencies. This is the tuning problem. It turns out that this problem can be solved by using ellipsoidal nanoparticles. In other words, for any negative value of dielectric permittivity $\epsilon_+^{(0)}$ an appropriate ellipsoidal nanoparticle can be found that will resonate for this value of permittivity and, consequently, for the corresponding value of frequency of optical radiation. It is also interesting that, for ellipsoidal nanoparticles, resonance permittivity values corresponding to uniform source-free electric fields (electrostatic approximation) can be found without resorting to the solution of integral equation (21). To demonstrate this, consider an ellipsoidal particle subject to a spatially uniform applied electric field $\mathbf{E}_{\text{ap}}$. The electric field $\mathbf{E}^+$ inside the particles is the superposition of the applied field and depolarizing field. The latter can be expressed in terms of polarization vector and depolarizing coefficients. This leads to the expression

$$\mathbf{E}^+ = \mathbf{E}_{\text{ap}} - \frac{1}{\epsilon_0}\hat{N}\mathbf{P}, \tag{95}$$

where $\mathbf{P}$ is the polarization vector, while $\hat{N}$ is (for the appropriate choice of axes) a diagonal matrix of depolarizing coefficients. By using the relation

$$\mathbf{P} = (\epsilon_+^{(0)} - \epsilon_0)\mathbf{E}^+, \tag{96}$$

formula (95) can be transformed as follows:

$$\mathbf{E}^+ + \frac{\epsilon_+^{(0)} - \epsilon_0}{\epsilon_0}\hat{N}\mathbf{E}^+ = \mathbf{E}_{\text{ap}}. \tag{97}$$

From Eq. (97) we find that the source-free and spatially uniform electric fields $\mathbf{E}^+$ inside the ellipsoidal nanoparticle must satisfy the homogeneous equations

$$\left(\hat{I} + \frac{\epsilon_+^{(0)} - \epsilon_0}{\epsilon_0}\hat{N}\right)\mathbf{E}^+ = 0, \tag{98}$$

where $\hat{I}$ is the identity matrix. Nonzero solution of Eq. (98) exist for such values of $\epsilon_+^{(0)}$ that the diagonal matrix $\hat{I} + [(\epsilon_+^{(0)} - \epsilon_0)/\epsilon_0]\hat{N}$ is singular. It follows now that spatially uniform in V^+ electrostatic (plasmon) resonances may exist only for the special values of permittivity of ellipsoidal nanoparticles given by the formula

$$\epsilon_{+i}^{(0)} = \epsilon_0\left(1 - \frac{1}{N_i}\right) \quad (i = 1,2,3), \tag{99}$$

where N_i are diagonal entries of $\hat{N}$.

It follows from the orthogonality conditions (32) that for all other electrostatic (plasmon) resonance modes the mean values of electric field components in V^+ are equal to zero. For this reason, all other resonance modes cannot be coupled to spatially uniform incident radiation.

It is apparent from Eq. (99), that for any negative value of $\epsilon_+^{(0)}(\omega)$ an ellipsoidal nanoparticle of appropriate aspect ratio (appropriate N_i) can be found that will resonate for this negative value of permittivity. Namely,

$$N_i = \frac{\epsilon_0}{\epsilon_0 - \epsilon_{+i}^{(0)}}. \tag{100}$$

In the case of the dispersion relation (62), the last assertion means that any frequency $\omega < \omega_p$ can be a resonance frequency for an appropriate ellipsoidal nanoparticles. Finally, from the dispersion relation (62), formula (99), and the well-known condition $\Sigma_i N_i = 1$ it follows that

$$\sum_i \omega_i^2 = \omega_p^2, \tag{101}$$

where ω_i are the resonance frequencies "along" the main axes.

It is worthwhile to mention that spherical nanoparticles can also be used for tuning. For instance, by controlling the gap between two spherical nanoparticles, tuning can be accomplished. This will be presented in the next section by using numerical simulations based on integral equation (21).

Next, we proceed to the brief discussion of tunability and optical controllability of electrostatic (plasmon) resonances in semiconductor nanoparticles. Semiconductors, like metals, may exhibit dispersion of the dielectric permittivity and its real part may assume negative values in the optical frequency range below the plasma frequency ω_p.[35] For the common dispersion relation (62), the plasma frequency is given by the formula

$$\omega_p^2 = \frac{n_e e^2}{\epsilon_0 m_e}, \tag{102}$$

where n_e is the conduction electron density, while other notations have their usual meaning.

The last formula clearly suggests that the dispersion relations $\epsilon_+(\omega)$ and, consequently, plasmon resonances can be controlled through manipulation of conduction electron density n_e. In semiconductors, the manipulation of conduction electron density can be accomplished by doping as well as by optical and depletion means. Indeed, by appropriate doping of semiconductor nanoparticles, the wide range of controllability of ω_p can be achieved and, in this way, the semiconductor nanoparticles can be tuned to resonate at desirable frequencies. The optical controllability is especially attractive because it can be utilized for the development of nanoscale light switches and all-optical nanotransistors. In these devices, one light beam can be used to generate conduction electrons and, in this way, to drive semiconductor nanoparticles into conditions when plasmon resonances can be excited by another light beam (see Fig. 4). Such materials as InSb may be especially attractive for the purpose of optical controllability of plasmon resonances because of their direct and small energy gap. An example of calculations of plasmon resonances in InSb nanoparticles is given in the next section. If the light gating of plasmon resonances can be realized, then semiconductors may well play a role in nanophotonics similar to what they do in electronics.

We conclude this section with a brief discussion of a plausible explanation of the phenomenon of ball lightning that is based on electrostatic (plasmon) resonances. The enigmatic natural phenomenon of ball lightning usually occurs after a

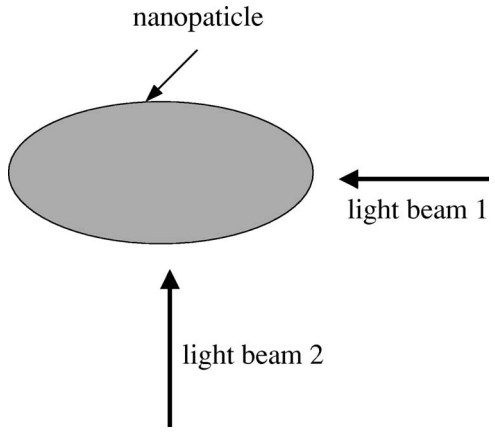

FIG. 4. Optical control of plasmon resonances: beam 2 is used for controlling of conduction electron density, while beam1 is used for excitation of plasmon resonances.

lightning strike that may lead to plasma formation and serve as a source of considerable electromagnetic radiation.[36,37] If the frequency spectrum of this radiation is such that the dielectric permittivity of the formed plasma is negative, then electrostatic (plasmon) resonances may occur. The nucleation of these resonances and the spatial growth of resonance regions may be facilitated by the scale invariance of the resonance frequencies. Electrostatic resonances may produce a considerable localized accumulation of electromagnetic energy that may visually manifest itself as ball lightning. Thus, the notion of electrostatic (plasmon) resonances may provide plausible explanations for energy accumulation in the ball lightning and its nucleation.

VI. NUMERICAL TECHNIQUE AND COMPUTATIONAL RESULTS

Now we proceed to the discussion of an efficient numerical technique for the solution of integral equation (21). To this end, let us partition S into N small pieces ΔS_j and rewrite integral equation (21) as follows:

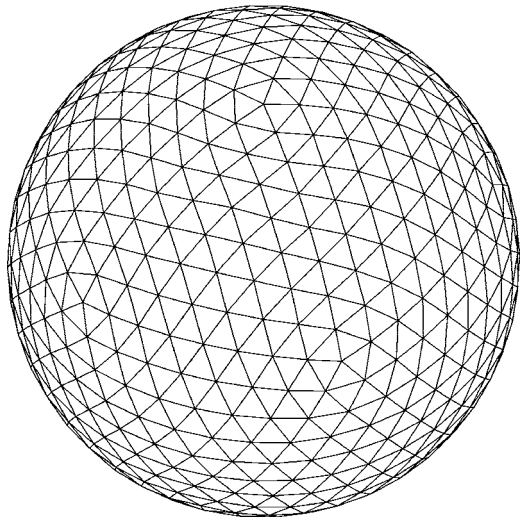

FIG. 5. Mesh for nanosphere.

TABLE II. Eigenvalues for a single nanosphere.

Mode number	Computed eigenvalues	Mie theory	Mode number	Computed eigenvalues	Mie theory
1	2.999191	3	21	9.038890	9
2	2.999193	3	22	9.049236	9
3	2.999194	3	23	9.049301	9
4	4.980130	5	24	9.049312	9
5	4.980130	5	25	10.86267	11
6	4.980148	5	26	10.86268	11
7	5.022817	5	27	10.86291	11
8	5.022828	5	28	10.94108	11
9	6.927911	7	29	10.94200	11
10	6.981790	7	30	11.03838	11
11	6.981884	7	31	11.03839	11
12	6.981885	7	32	11.03846	11
13	7.027287	7	33	11.06465	11
14	7.027289	7	34	11.06497	11
15	7.027393	7	35	11.06500	11
16	8.915480	9	36	12.75603	13
17	8.915606	9	37	12.84736	13
18	8.915633	9	38	12.84819	13
19	8.979679	9	39	12.84824	13
20	8.979774	9	40	12.93150	13

$$\sigma(Q) = \frac{\lambda}{2\pi}\sum_{j=1}^{N}\int_{\Delta S_j}\sigma(M)\frac{\mathbf{r}_{MQ}\cdot\mathbf{n}_Q}{r_{MQ}^3}dS_M. \tag{103}$$

Now, we integrate Eq. (103) over ΔS_i:

$$\int_{\Delta S_i}\sigma(Q)dS_Q = \frac{\lambda}{2\pi}\sum_{j=1}^{N}\int_{\Delta S_j}\sigma(M)\left[\int_{\Delta S_i}\frac{\mathbf{r}_{MQ}\cdot\mathbf{n}_Q}{r_{MQ}}dS_Q\right]dS_M \quad (i=1,2,\ldots,N). \tag{104}$$

By introducing notations

$$\omega_i(M) = \int_{\Delta S_i}\frac{\mathbf{r}_{MQ}\cdot\mathbf{n}_Q}{r_{MQ}^3}dS_Q, \tag{105}$$

the last formula can be presented as follows:

TABLE III. Eigenvalues for a single nanoellipsoid.

Mode number	Computed eigenvalues	Theoretical values	Mode number	Computed eigenvalues
1	1.976541	1.9723	6	4.590262
2	3.335450		7	4.829570
3	4.080630	4.0507	8	5.645674
4	4.080692	4.0570	9	5.645746
5	4.590155		10	6.314742

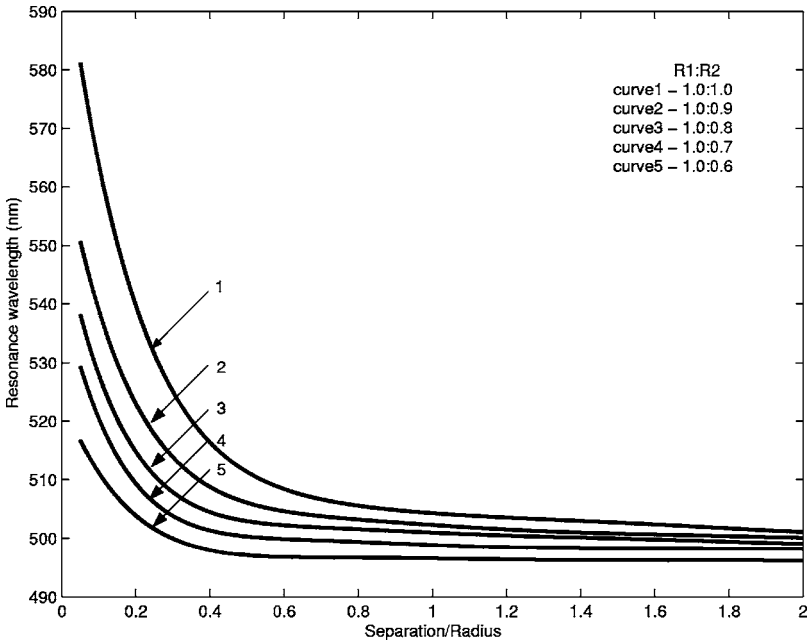

FIG. 6. Resonance wavelength for two nanospheres on substrate.

$$\int_{\Delta S_i} \sigma(Q) dS_Q = \frac{\lambda}{2\pi} \sum_{j=1}^{N} \int_{\Delta S_j} \sigma(M) \omega_i(M) dS_M. \quad (106)$$

It is apparent that $\omega_i(M)$ is the solid angle which ΔS_i subtends at point M. By introducing new variables

$$X_i = \int_{\Delta S_i} \sigma(Q) dS_Q, \quad (107)$$

integrals in the right-hand side of Eq. (106) can be approximated as follows:

$$\int_{\Delta S_j} \sigma(M) \omega_i(M) dS_M \approx \omega_i(M_j) X_j = \omega_{ij} X_j, \quad (108)$$

where M_j is some middle point of partition ΔS_j. It is apparent (on intuitive grounds) that approximation (108) is more accurate than direct discretization of integral in Eq. (21), because solid angles $\omega_i(M)$ are smooth functions of M, while the kernel of integral equation (21) is (weakly) singular. By substituting formulas (107) and (108) into Eq. (106), we obtain

$$X_i = \frac{\lambda}{2\pi} \sum_{j=1}^{N} \omega_{ij} X_j. \quad (109)$$

Another advantage of discretization (109) is that the evaluation of singular integrals in calculations of ω_{ii} can be completely avoided. Indeed, according to formulas (31) and (105), we find

$$\omega_{ii} \approx 2\pi - \sum_{i=1, i \neq j}^{N} \omega_{ij}. \quad (110)$$

The numerical technique based on discretization (109) has been software implemented and extensively tested. It has proved to be remarkably accurate, even for calculations of large eigenvalues. This technique is illustrated by the examples presented below.

The algorithm described above has been first tested for spherical particles where exact analytical solutions are available (Mie theory[33]). The mesh used in calculations is shown in Fig. 5, while the results of numerical computations are presented in Table II. It is apparent from this table that numerical results are quite accurate even for appreciably high mode orders. Next, the described algorithm has been tested for ellipsoidal nanoparticles. The computational results are presented in Table III for the case of ellipsoid of revolution

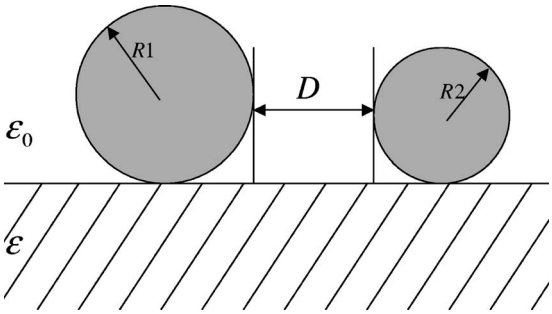

FIG. 7. Two nanospheres on substrate.

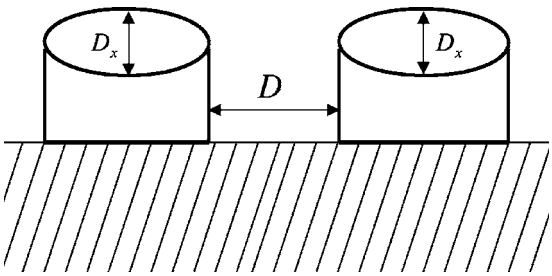

FIG. 8. Ellipsoidal cylinders on substrate.

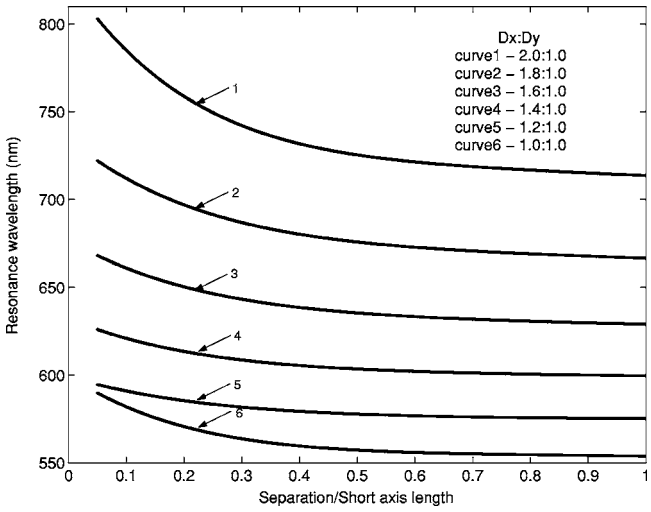

FIG. 9. Resonance wavelength for two ellipsoidal cylinders on substrate.

TABLE IV. Comparison with experimental results (Ref. 39) for gold nanoring.

	Ring1	Ring2	Ring3
Outer radius of the ring (nm)	60	60	60
Height of the ring (nm)	40	40	40
Thickness of ring wall (nm)	14(2)	10(2)	9(2)
Experimental resonance (nm)	1000	1180	1350
Computational resonance (nm)	940	1102	1214

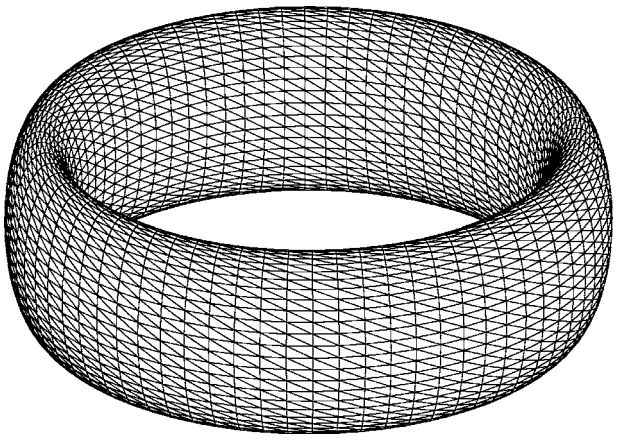

FIG. 10. Mesh for nanoring.

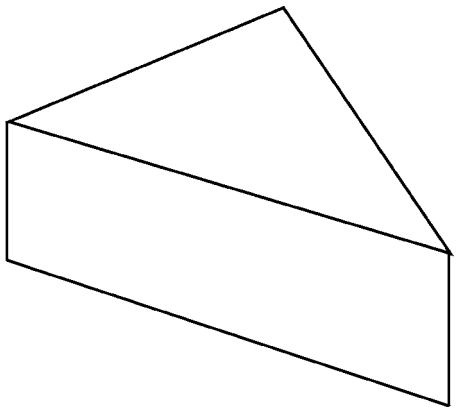

FIG. 11. Triangular nanoprism.

with the main axis ratios 1:1:1.55. It is evident from this Table that the computed eigenvalues compare quite well with the exact (theoretical) eigenvalues $\lambda_i = 1/(1-2N_i)$ for spatially uniform modes [see formula (99)]. It is also apparent that for those modes $\Sigma_i(1/\lambda_i)$ is very close to 1 as it must be.

Figure 6 presents the computational results for the resonant free-space wavelength as a function of separation distance between two gold spherical nanoparticles located on a dielectric substrate with $\epsilon = 2.25\epsilon_0$ for different values of radius ratio (see Fig. 7). The dispersion relation for gold published in Ref. 38 has been used in calculations. It is clear from Fig. 6 that the separation between two spheres can be effectively used for tuning of plasmon resonances to desirable frequencies. Figure 6 is an example of our numerous computations performed for two and several nanospheres of various radii and separation distances. These results are not presented here due to the lack of space and will be published elsewhere.

We have computed resonance wavelength for two short gold cylinders of ellipsoidal cross sections placed on a dielectric substrate (see Fig. 8). Figure 9 presents the computational results for resonance wavelength as the function of separation between cylinders for different values of axis ratio.

Table IV presents the computational results for gold nanorings placed on a dielectric substrate. In this table, the computational results for resonance wavelengths are compared with those found experimentally (see Ref. 39). The mesh used in calculations is shown in Fig. 10. We have also compared our numerical results with available experimental data for the following two cases: a) a short gold cylinder of ellipsoidal cross section (with long axis 130 nm, short axis 84 nm, height 30 nm) placed on a dielectric substrate and b) a gold triangular nanoprism (with edge length 48 nm, height

TABLE V. Comparison with experimental results (Refs. 40 and 41) for gold ellipsoidal cylinder and triangular prism.

Resonance wavelength	Cylinder (nm)	Prism (nm)
Computational results	622	653
Experimental results	645	690

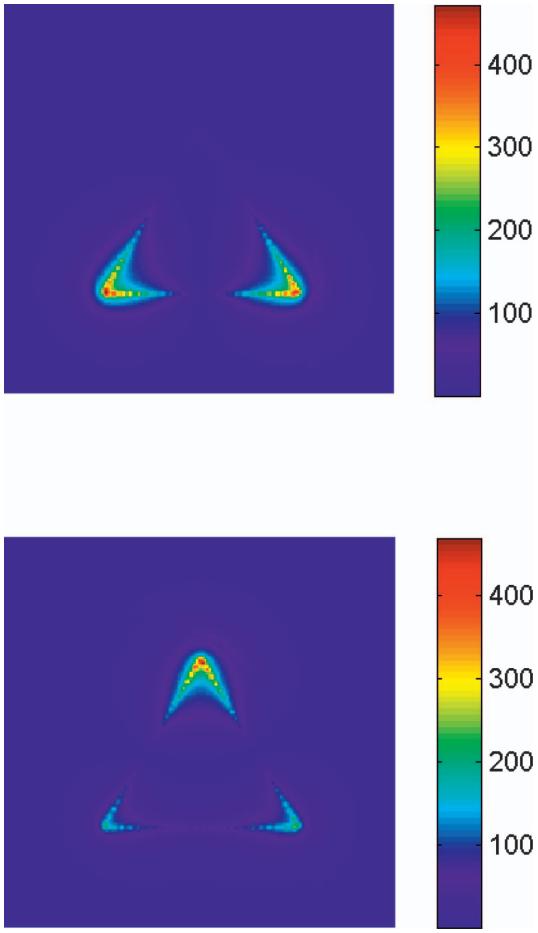

FIG. 12. (Color) Electrical field of first two resonance modes for triangular nanoprism.

14 nm) (Fig. 11). Table V presents the comparison between our computational results and experimental data published in references,[40,41] respectively. The electrical field of the resonance mode for gold triangle prism is shown in Fig. 12. In all above computations, the dispersion relation for gold[38] has been used.

Finally, Fig. 13 presents simulation results of the extinction cross-section of a InSb nanosphere placed on a glass substrate with permittivity $2.25\epsilon_0$. [The technique for computations of extinction cross-sections is based on the solution of inhomogeneous integral equations of the type (21) and (27) and will be discussed elsewhere.] The intrinsic dispersion relation of InSb used in calculations was taken from Ref. 35. It is apparent that the presented computational results compare quite well with known theoretical results and are in a reasonably good agreement with the available experimental data.

VII. CONCLUSION

A boundary integral equation technique for the direct calculation of resonance frequencies of nanoparticles of arbitrary shapes is discussed. In electrostatic approximation, this technique is based on the solution of eigenvalue problem for the specific boundary integral equation. General physical properties of electrostatic (plasmon) resonances are studied and strong orthogonality properties of resonance modes, two-dimensional phenomena of "twin" spectrum and explicit estimates of the resonance spectrum range in terms of geometric characteristics of convex nanoparticles are reported. Second-order corrections for resonance values of dielectric permittivity in terms of free-space wavelength are derived by using the mathematical machinery of boundary integral

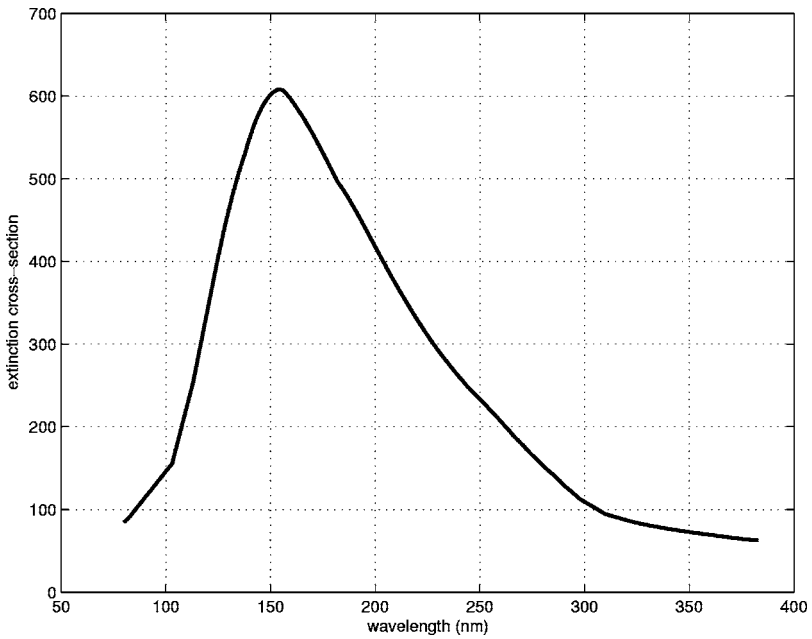

FIG. 13. Computational extinction cross-section of single InSb nanosphere placed on a glass substrate ($\epsilon=2.25\epsilon_0$).

equations. Tunability and optical controllability of plasmon resonances in semiconductor nanoparticles are discussed and, as a digression, a plausible explanation for nucleation and formation of ball lightning based on electrostatic (plasmon) resonances is outlined. An efficient numerical algorithm for the calculation of resonance frequencies is developed and illustrated by extensive computational results that are compared with available experimental data.

[1] T. J. Silva and S. Schultz, Rev. Sci. Instrum. **67**, 715 (1996).
[2] R. M. Stockle, Y. D. Suh, V. Deckert, and R. Zenobi, Chem. Phys. Lett. **318**, 131 (2000).
[3] J. C. Hulteen, D. A. Treichel, M. T. Smith, M. L. Duval, T. R. Jensen, and R. P. V. Duyne, J. Phys. Chem. B **103**, 3854 (1999).
[4] R. Elghanian, J. J. Storhoff, R. C. Mucic, R. L. Letsinger, and C. A. Mirkin, Science **277**, 1078 (1997).
[5] S. Schultz, D. R. Smith, J. J. Mock, and D. A. Schultz, Proc. Natl. Acad. Sci. U.S.A. **97**, 996 (2000).
[6] J. P. Kottmann, O. J. F. Martin, D. R. Smith, and S. Schultz, Chem. Phys. Lett. **341**, 1 (2001).
[7] M. Moskovits, Rev. Mod. Phys. **57**, 783 (1985).
[8] S. Nie and S. R. Emory, Science **275**, 1102 (1997).
[9] H. Xu, E. J. Bjerneld, M. Kall, and L. Borjesson, Phys. Rev. Lett. **83**, 4357 (1999).
[10] J. R. Krenn, A. Dereux, J. C. Weeber, E. Bourillot, Y. Lacroute, J. P. Goudonnet, G. Schider, W. Gotschy, A. Leitner, F. R. Aussenegg, and C. Girard, Phys. Rev. Lett. **82**, 2590 (1999).
[11] J. C. Weeber, A. Dereux, C. Girard, J. R. Krenn, and J. P. Goudonnet, Phys. Rev. B **60**, 9061 (1999).
[12] T. Yatsui, M. Kourogi, and M. Ohtsu, Appl. Phys. Lett. **79**, 4583 (2001).
[13] J. Tominnaga, C. Mihalcea, D. Buchel, H. Fukuda, T. Nakano, N. Atoda, H. Fuji, and T. Kikukawa, Appl. Phys. Lett. **78**, 2417 (2001).
[14] J. Tominnaga, T. Nakano, and N. Atoda, Proc. SPIE **3467**, 282 (1999).
[15] L. Men, J. Tominaga, Q. C. H. Fuji, and N. Atoda, Proc. SPIE **4085**, 204 (2001).
[16] M. R. Pufall, A. Berger, and S. Schultz, J. Appl. Phys. **81**, 5689 (1997).
[17] J. P. Kottmann, O. J. F. Martin, D. R. Smith, and S. Schultz, Phys. Rev. B **64**, 235402 (2001).
[18] J. P. Kottmann, O. J. Martin, D. R. Smith, and S. Schultz, J. Microsc. **202**, 60 (2001).
[19] J. J. Mock, M. Barbic, D. R. Smith, D. A. Schultz, and S. Schultz, J. Chem. Phys. **116**, 6755 (2002).
[20] F. Ouyang and M. Isaacson, Philos. Mag. B **60**, 481 (1989).
[21] F. Ouyang and M. Isaacson, Ultramicroscopy **31**, 345 (1989).
[22] F. J. GarciadeAbajo and J. Aizpurua, Phys. Rev. B **56**, 15 873 (1997).
[23] F. J. GarciadeAbajo and A. Howie, Phys. Rev. Lett. **80**, 5180 (1998).
[24] D. R. Fredkin and I. D. Mayergoyz, Phys. Rev. Lett. **91**, 253902 (2003).
[25] O. D. Kellogg, *Foundations of Potential Theory* (McGraw-Hill, New York, 1929).
[26] S. G. Mikhlin, *Mathematical Physics, an Advanced Course* (North-Holland, Amsterdam, 1970).
[27] O. Tozoni and I. Mayergoyz, *Analysis of 3D Electromagnetic Fields* (Techuika, Kyiv, 1974).
[28] I. Mayergoyz, *Iterative Techniques for the Analysis of Static Fields in Inhomogeneous, Anisotropic and Nonlinear Media* (Naukova Dumka, Kyiv, 1976).
[29] M. I. Stockman, S. V. Faleev, and D. J. Bergman, Phys. Rev. Lett. **87**, 167401 (2001).
[30] K. Li, M. I. Stockman, and D. J. Bergman, Phys. Rev. Lett. **91**, 227402 (2003).
[31] W. Blaschke, *Kreis und Kugel* (Auflage, Berlin, 1956).
[32] G. Y. Lyubarskii, *Application of Group Theory in Physics* (Pergamon Press, New York, 1960).
[33] C. F. Bohren and D. R. Huffman, *Absorption and Scattering of Light by Small Particles* (John Wiley, New York, 1983).
[34] J. D. Jackson, *Classical Electrodynamics* (John Wiley, New York, 1999).
[35] E. D. Palik, *Handbook of Optical Constant of Solids* (Academic Press, New York, 1985).
[36] P. L. Kapitsa, Dokl. Akad. Nauk SSSR **101**, 245 (1955).
[37] Y. H. Ohtsuki and H. Ofuruton, Nature (London) **350**, 139 (1991).
[38] P. B. Johnson and R. W. Christy, Phys. Rev. B **6**, 4370 (1972).
[39] J. Aizpurua, P. Hanarp, D. S. Sutherland, M. Kall, G. W. Bryant, and F. J. GarciadeAbajo, Phys. Rev. Lett. **90**, 057401 (2003).
[40] K. H. Su, Q. H. Wei, X. Zhang, J. J. Mock, D. R. Smith, and S. Schultz, Nano Lett. **3**, 1087 (2003).
[41] E. Hao, G. C. Schatz, and J. T. Hupp, J. Fluoresc. **14**, 331 (2004).